Microgravity Science and Technology (2018) 30:943–949
https://doi.org/10.1007/s12217-018-9655-0

ORIGINAL ARTICLE

A Comparative Study of Near-Limit Flame Spread Over a Thick Solid in Space- and Ground-Based Experiments

Feng Zhu[1,2] · Shuangfeng Wang[1,2] · Zhanbin Lu[3]

Received: 31 March 2018 / Accepted: 7 September 2018 / Published online: 2 October 2018

Abstract

Microgravity experiments have been performed aboard the SJ-10 satellite of China to investigate flame spread behaviors over a thick PMMA in low-velocity opposed flow. Two variables are considered: opposed-flow velocity in a range of 0 to 9 cm/s, and ambient oxygen concentration in a range of 25% to 50%. It is found that, when the flow velocity is reduced, the initial extended flame may breaks into separate flamelets after a dynamic transition process. This is the first observation of the flamelets spreading over a thick solid fuel in microgravity. Flame and flamelet propagate with a steady spread rate, which increases with the increasing flow velocity and oxygen concentration. A flammability map using oxygen concentration and flow velocity as coordinates is established, which delineates the uniform regime, the flamelet regime, and extinguished regime. The flammability boundary was extended to lower oxygen concentrations and lower flow velocities by the flamelet regime. The microgravity results are compared with the counterparts in ground-based narrow channel apparatus (NCA) experiments. Results showed that although the NCA tests overestimate the flame spread rate and flammable area, also exhibit differences in detailed flamelet formation process, flame and flamelet behaviors agree well with that in microgravity in a qualitative manner.

Keywords Flame spread · Extinction limit · Thick solid · Microgravity · Opposed flow · Narrow channel apparatus

Introduction

Motivated primarily by the fire safety concerns for inhabited spacecraft, flame spread over non-metallic solid fuel in microgravity has been studied for several decades (e.g., the reviews of T'ien et al. 2001 and Fujita 2015). From the viewpoint of fundamental understanding of flame spread, microgravity experiments are also of interest to researchers because a purely forced-convective oxidizer flow can be generated, and therefore flame behaviors in low-velocity flow regime could be examined. Most microgravity experiments of flame spread, however, have been concerned with thermally-thin fuels (T'ien et al. 2001). The ignition of a thick solid and subsequent transition to flame spread has a relatively long time scale, which makes the observation of flame spread difficult in ground-based microgravity facilities such as drop towers. This highlights the need for long-duration microgravity experiments in space to reveal the combustion processes of thermally-thick solids, while the opportunity to perform space-based experiments has been scarce.

Experimental results for thick solid combustion in microgravity were first obtained aboard space shuttle missions (West et al. 1996). In these experiments, flame spread over thick PMMA samples was examined in quiescent environments of 50% O_2 at 1 atm, 50% O_2 at 2 atm, and 70% O_2 at 1 atm, respectively. The results showed that, within the experimental period, all flames were unsteady with the spread rate slowly decreasing with time. In a later space experiment during a space shuttle flight, a longer PMMA sample was burned in a quiescent environment of 50% O_2 at 1 atm to determine the ultimate fate

This article belongs to the Topical Collection: Approaching the Chinese Space Station - Microgravity Research in China
Guest Editors: Jian-Fu Zhao, Shuang-Feng Wang

✉ Shuangfeng Wang
sfwang@imech.ac.cn

1 Key Laboratory of Microgravity, Institute of Mechanics, Chinese Academy of Sciences, Beijing 100190, China

2 School of Engineering Science, University of Chinese Academy of Sciences, Beijing 100049, China

3 Institute of Applied Mathematics and Mechanics, Shanghai University, Shanghai 200072, China

of the flame (Altenkirch et al. 1998). After ignition, the flame was observed to sustain for approximately 540 s, and eventually flame extinction occurred. Such an inherently unsteady flame in a quiescent microgravity environment was also captured by numerical modeling (West et al. 1996; Altenkirch et al. 1998), which further predicted this behavior for oxygen concentrations up to 100% at 1 atm. Two sounding rocket experiments have been conducted to investigate the effects of flow velocity on flame spread over thermally-thick PMMA (Vietoris et al. 2000; Olson et al. 2004). In the experiment of Vietoris (2000), the sample was ignited in 40% O_2 at a flow velocity of 15 cm/s, and the velocity was then decreased to 10 cm/s and finally to 5 cm/s. A stable opposed-flow flame was observed to spread in the relatively fast flows, whereas the flame spread ceased at the flow velocity of 5 cm/s. The analysis showed that the three different flow conditions correspond to strong flame spread, transitional and extinction regimes, respectively. The other sounding rocket experiment (Olson et al. 2004) extended the oxygen concentration conditions to 35% O_2, 50% O_2, and 70% O_2 while keeping a low external flow velocity ($\leq$ 10 cm/s) for each test. Steady flame spread opposing the flow was found in 50% O_2 and 70% O_2 at 1 cm/s, and in 35% O_2 at 5 and 10 cm/s, although the flame extinguished in 35% O_2 at 1 cm/s.

In normal gravity experiments, Zhu et al. (2016) and Wang et al. (2016a) made an attempt to access the flame propagation and extinction phenomena for a thick PMMA in low-velocity gas flows. By employing a narrow channel apparatus (NCA) to suppress buoyant flow, the flame spread behavior was examined as a function of the velocity and oxygen concentration of the forced flow, and a flammability map using oxygen concentration and flow velocity as coordinates was plotted. Although the narrow-channel type apparatus has been utilized by various authors to reproduce essential features of microgravity flame spread for thermally-thin fuels (Ivanov et al. 1999; Olson et al. 2009; Zhang and Yu 2011), it was noted that for thick fuels more microgravity experimental data are needed to validate the NCA test results.

This paper describes the results of a space-based microgravity experiment on flame spread over thermally-thick PMMA. The experiment was conducted aboard the SJ-10 satellite of China in April 2016 (Hu et al. 2014; Zhao et al. 2016). For varying low-velocity opposed-flow and ambient oxygen concentration, detailed observations of the flame behavior are presented. Moreover, the experimental results are compared with the counterparts in normal gravity NCA tests, and the NCA facility is evaluated for its performance in producing a microgravity flame spread environment for thick solid fuels.

Experimental

Microgravity Experiments

A payload was specifically designed for the space experiment "Ignition and Burning of Solid Materials in Microgravity" conducted aboard the SJ-10 satellite. The flight hardware is shown in Fig. 1a. Eight flow tunnels, which have an identical cross section of 95 mm × 95 mm and a length of 120 mm, are installed inside a 39-L combustion chamber. Four of the tunnels are used for experiments of opposed-flow flame spread over thick PMMA plate, and it is for these experiments that the results are reported in this paper. Each of the four flow tunnels accommodates an aluminum sample holder. A PMMA plate, 61.6 mm long × 50 mm wide × 10 mm thick, is embedded in the sample holder, with the plate surface flushing with the holder, and insulated from the holder by using ∼1-mm-thick mica plates. The igniter is a resistively heated wire embedded in the fuel sample 15.8 mm away from the downstream edge. The forced gas flow in the flow tunnel is driven by a fan installed at the downstream end of the tunnel. The bulk cold flow velocity, calibrated using a Laser Doppler Velocimeter (LDV) on ground, can be adjusted in a range of 0 to 12 cm/s, and the smoothness of the flow is verified by means of smoke flow visualization in ground tests. A Schematic of the flow tunnel and sample holder is shown in Fig. 1b.

An integrated gas control module, comprising a gas supply submodule and a gas release submodule, serves to establish the specified oxidizer atmosphere in the combustion chamber. The gas supply submodule has two 2.1-L gas bottles that are charged with 21% O_2/79% N_2 and 50% O_2/50%N_2mixtures, respectively, up to 13.5 MPa. So, by blending the two mixtures at an appropriate ratio, an O_2/N_2 mixture could be obtained in the oxygen concentration range of 25% and 50%. Before each test, the gas release submodule works first, and residual gas in the combustion chamber is vented to the vacuum of outer space. Once the chamber pressure decreases below 0.5 kPa, gas from one bottle (charged with 21% O_2/79% N_2) is filled into the chamber until a preset pressure is reached, and then the chamber is further charged by gas from another bottle until the chamber pressure reaches 101 kPa. After the gas filling operations, all the fans inside the chamber are turned on for 8 minutes to blend the mixtures thoroughly. The mixture blending procedure establishes an initial flow condition throughout the test flow tunnel as well. During the experiments, the chamber pressure and oxygen concentration are constantly monitored by corresponding sensors, and the ambient temperature in the chamber is measured using a K-type thermocouple.

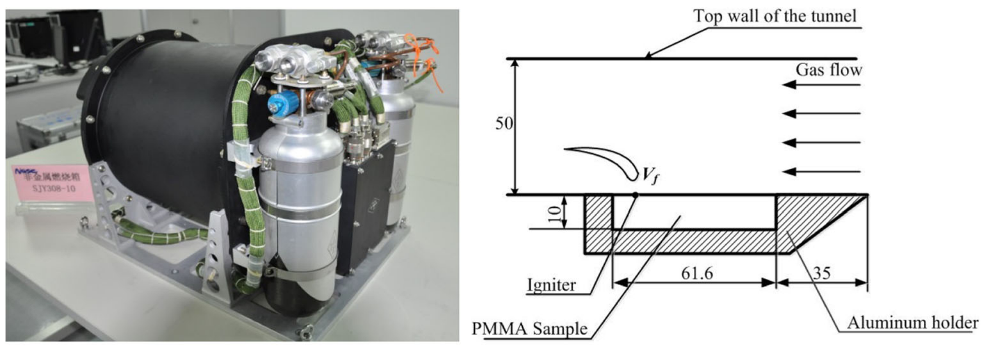

(a) (b)

Fig. 1 **a** Flight payload of Ignition and Burning of Solid Materials in Microgravity for SJ-10 satellite. **b** Schematic of the flow tunnel and sample holder

The four opposed-flow flame spread tests are conducted individually in order during the orbital flight mission. An oxygen concentration is specified for each test, which is 25%, 30%, 35%, and 40%, respectively. The experimental procedure, which is automatically controlled, is described as follows. Once the mixture blending procedure is complete, the initial flow with a velocity of 9 cm/s is established in the tunnel. Ignition is then accomplished by energizing the igniter for 20 s. After a prescribed period, the initial flow velocity is decreased to 6 cm/s, 3 cm/s, and finally to 0. Each flow velocity is kept at least for 40 s, which is long enough for the flame to reach its ultimate state. The flame behaviors are recorded by two color CCD cameras at a framing rate of 25 fps, one for top view and another side view through the two windows on the tunnel walls.

Just prior to the ignition, the measured chamber pressure comes within 101 ± 1.3 kPa, and the measured oxygen concentration shows a maximum deviation of 2.3% in respect to the desired value. The ambient temperature in the chamber depends on the environment inside the satellite, which is about 12 °C. It is found that the variation of the environment could be considered ignorable during all the combustion tests, with the maximum change occurring in the 40% case: a pressure rise of 1.4 kPa, oxygen content decrease of 2.1%, and ambient temperature increase of 3 °C.

Normal Gravity Experiments with the Narrow Channel Apparatus

The NCA experiments of flame spread over a thick fuel were described in detail by Zhu et al. (2016) and Wang et al. (2016a). Here a brief description is given for the completeness of the paper merely. The NCA consists mainly of a flow system and a horizontal flow channel, which has a vertical inner height of 10 mm. The top and side walls of the channel are made of quartz glass for visualization purpose. The flow system supplies desired oxidizer gas to the flow channel at a controlled flow rate. The velocity of the forced flow in the channel can be adjusted from 0 to 15 cm/s.

A PMMA plate, with a size of 60 mm long, 50 mm wide and 10 mm thick, is embedded in the aluminum floor of the flow channel. During the opposed flame spread test, the fuel is ignited by a resistively heated wire, which is mounted at the downstream end of the sample. Two color digital video cameras are used to record the flame behaviors with a frame rate of 25 fps, one for top view and the other for side view.

Results and Discussion

Description of Spreading Flames

Depending on the magnitude of the opposed flow and/or the ambient oxygen content, microgravity flames spreading over the PMMA samples are observed to take two different forms: uniform flame, which extends itself across the sample width with a continuous leading front; and flamelet, which means small, three-dimensional flames that are formed when a uniform flame can no longer be sustained and shrinks into individual flames separated by non-burning fuel. Uniform flames sustain at flow velocities of 9 cm/s and 6 cm/s in 40% O_2 and 35% O_2, respectively. When the flow velocity is slowed down to 3 cm/s in either oxygen atmospheres, the flame changes its apparent form into flamelets, which extinguish when the flow is stopped and a quiescent environment is achieved. In 30% O_2, no uniform flame is observed, and a single flamelet is established following the ignition transition. Although this flamelet survives as the flow velocity decreases to 6 cm/s, it goes to extinction at 3 cm/s. For the 25% O_2 case, the flame fails to spread and extinguishes in a short time although the sample is ignited successfully.

Top-view images of microgravity flames spreading in 40% O_2 at three different flow velocities (9 cm/s, 6 cm/s, and 3 cm/s) are shown in Fig. 2a. The flame is always pale blue, and the color is almost uniform. When the gas flow is decreases to 3 cm/s, the extended flame breaks up into two separate flamelets. The flame transition from a uniform flame to flamelets is shown in Fig. 3a by flame image sequence. As the flow velocity is reduced, the middle part of the uniform flame becomes dimmer and thinner, and then the flame is divided into two flamelets. The transition is a dynamic process, which is characterized by repeated connecting of flamelets and dividing of the united flame. The transition process persists approximately for 38 s, and finally quasi-stable flamelets are formed.

The flamelets shown in Fig. 3a are tracked to determine their widths and leading edge positions as a function of time, with that on the left marked as flamelet 1, and the right one flamelet 2. The widths of both flamelets during spreading are shown in Fig. 4a. After formation, each flamelet has an equal width of ∼ 15 mm. The time history of the leading edge position is shown in Fig. 5a. A linear position-time plot is clearly seen for each flamelet, indicating a constant spread rate for each of them. It is noted that, although the spread of the flamelet is steady, the flamelet width decreases very slowly in the available test time. For this reason, the flamelets are considered as only quasi-steady. The flamelets in 35% O_2 and 30% O_2 demonstrate similar behaviors to those in 40% O_2, but only one flamelet is formed in 35% O_2 when the flow velocity is reduced from 6 cm/s to 3 cm/s. So, flamelets seem to be a common flame spread mode for thick PMMA in low-velocity opposed flow. At this point, the microgravity experiments of Olson et al. (2004) should be noted that although the tests are performed at comparable

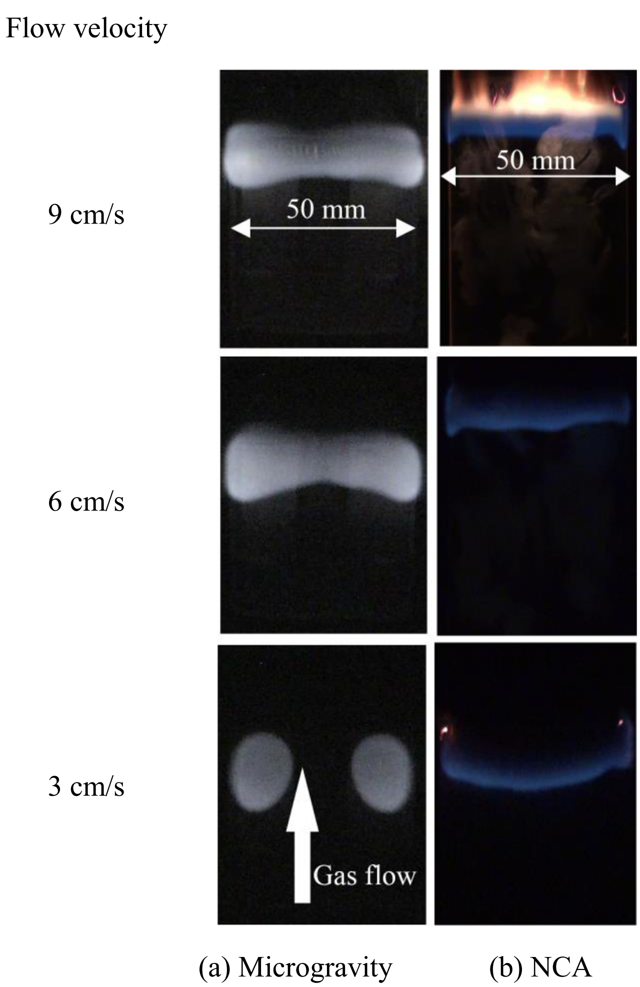

Fig. 2 Top view images of opposed-flow flames spreading in 40% O_2. **a** Microgravity experiment; **b** NCA experiment

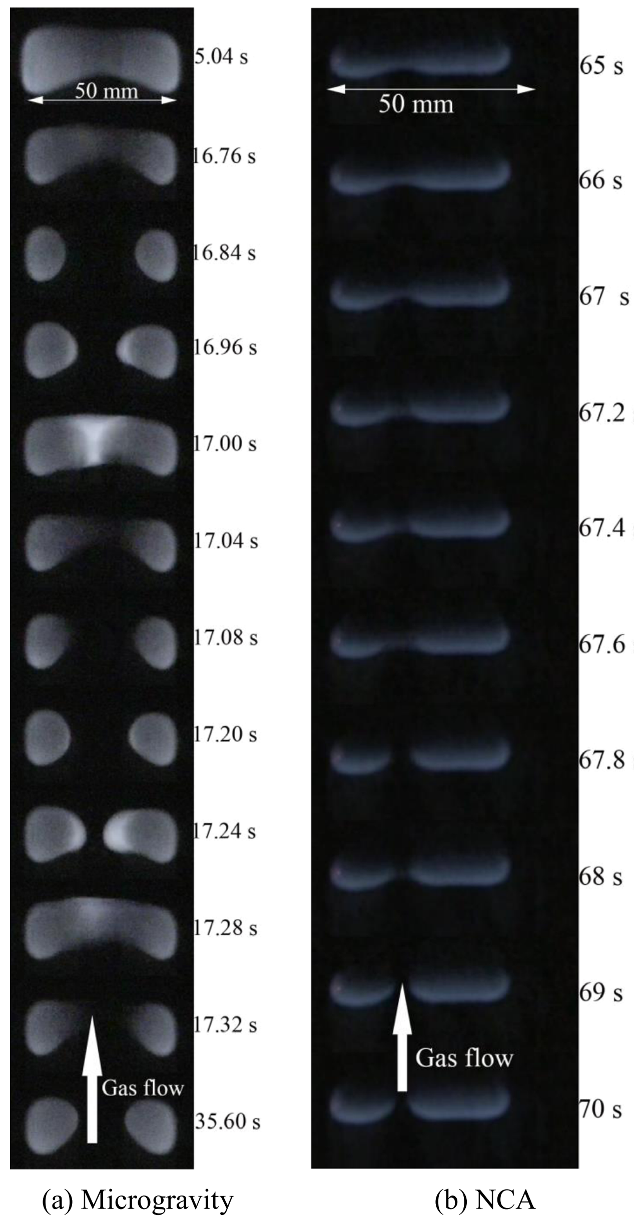

Fig. 3 A time sequence of images from microgravity and normal gravity experiments showing flame transition from a uniform flame to flamelets. **a** Microgravity experiment, in 40% O_2 at 3 cm/s; **b** NCA experiment, in 21% O_2, at 3 cm/s

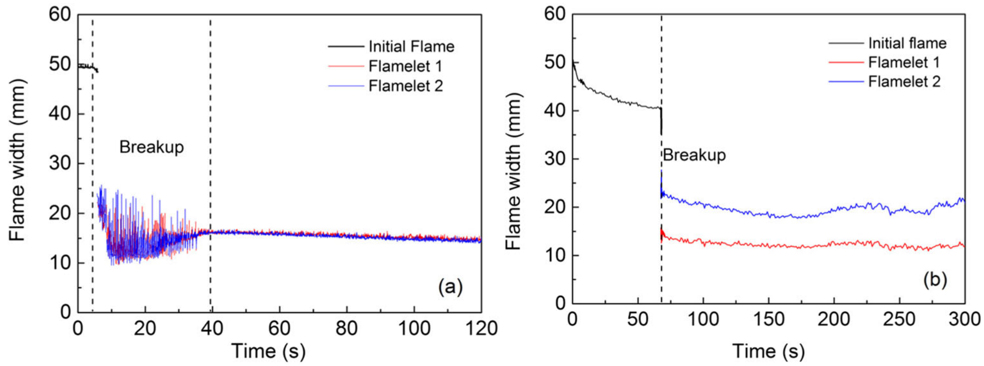

Fig. 4 Flame width as a function of time **a** Microgravity experiment; **b** NCA experiment

conditions, the flamelet was not observed on account of the narrow sample employed (6.35 mm), which precludes the formation of flamelet.

Results of the NCA experiments (Wang et al. 2016a; Zhu et al. 2016) are shown in Figs. 2b to 5b to compare with the counterparts in microgravity experiments. From Fig. 2b, it is seen that all flames in NCA have a bright blue-colored leading edge. At 9 cm/s, the flame length increases dramatically because a bright-yellow trailing tail begins to develop. A more important difference is found at 3 cm/s, where, unlike the microgravity case, a uniform flame survives in NCA. In fact, the flamelet region in NCA is much narrower than that in microgravity, and a lower oxygen concentration is needed to make a flamelet occur in NCA. Figure 3b shows the flame transition from a uniform flame to flamelets in 21% O_2. In this NCA test, the sample is ignited at 4 cm/s, and then the flow is decreased to 3 cm/s. As the flow is reduced, the flame leading edge became corrugated. Within $\sim$1 s, the flame divides into two flamelets. The flame transition advances gradually, and the flame oscillation phenomena observed in microgravity experiments do not appear. Flamelets over thick PMMA were first found by Matsuoka et al. (2017) in normal gravity experiments of flame spread in a narrow gap between two PMMA plates. The formation of flamelets, which emerges exclusively near the quenching limit, is believed to result from thermal-diffusive instability of the diffusion flame (Wang et al. 2016b). With the approach of the gas flow velocity to the quenching limit, radiative heat loss plays a progressively more important role. As a result, the diffusion flame is no longer able to sustain a uniform flame front and splits into discrete reaction cells after the onset of instability. The reaction cells close themselves and eventually form into the transversely distributed flamelets. Note that similar cellular instability also occurs in spreading diffusion flames over thin solid fuels (Olson et al. 2009; Wang et al. 2016b). Flame width and leading edge position in NCA as a function of time are shown in Figs. 4b and 5b respectively. It can be seen that in the NCA experiment, each flamelet has a constant width and spread rate.

Flammability Map

The present microgravity results, supplemented with existing data from other groups (Olson et al. 2004; Altenkirch et al. 1998; West et al. 1996), are used to establish a flammability map for flames spreading over PMMA sheet. As shown in Fig. 6, the map delineates regimes of flame spread modes as a function of oxygen concentration and opposed flow velocity. The flammable area of the map is divided into two different regions, i.e. uniform flame and flamelets. For a given oxygen concentration, the uniform flame breaks into flamelets as the flow velocity decreases, and flamelets extinguish eventually at sufficiently low velocities. With a

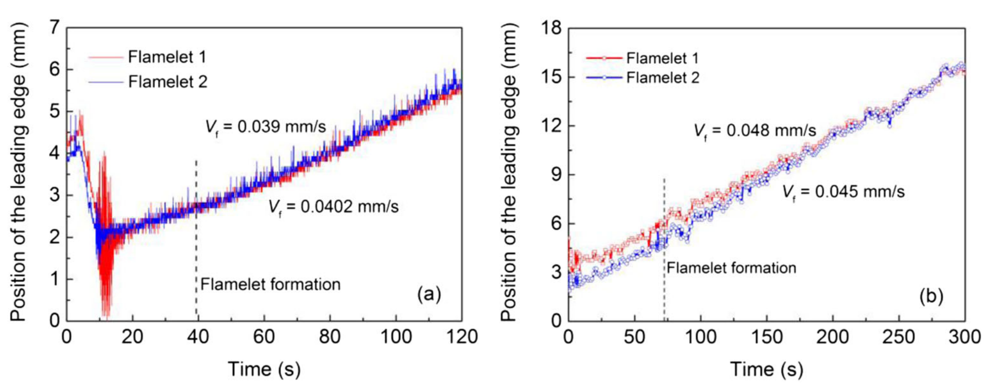

Fig. 5 Position of flame leading edge as a function of time **a** Microgravity experiment **b** NCA experiment

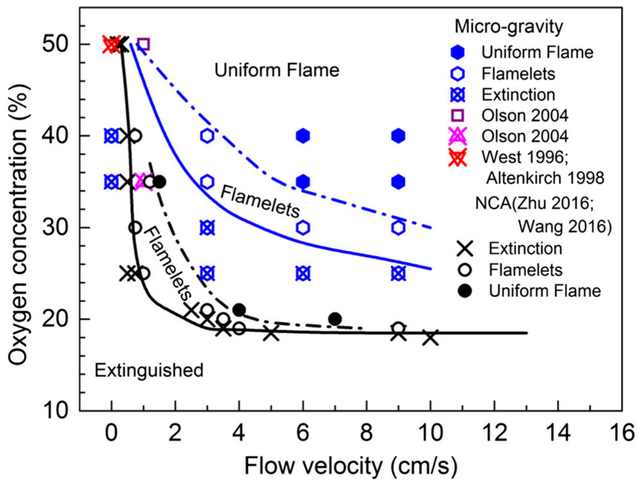

Fig. 6 Flammability map for thick PMMA in microgravity and NCA experiments

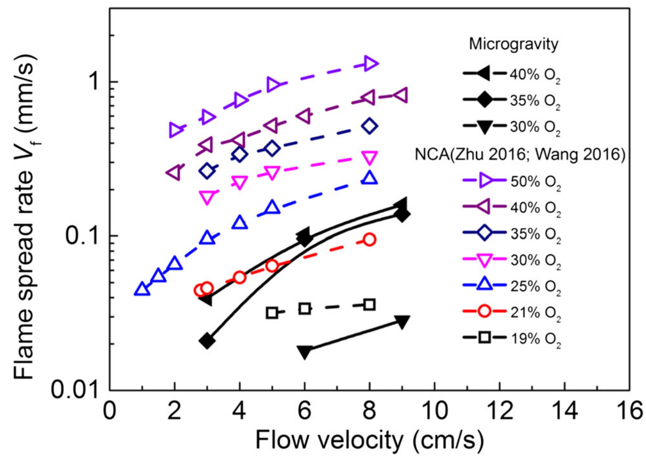

Fig. 7 Flame spread rates in microgravity and NCA experiments as a function of flow velocity at different oxygen concentrations

given flow velocity, as the oxygen concentration decreases, the same sequence of events occurs. It is obvious that the range of material flammability is extended by the flamelet regime. A flamelet can sustain at lower opposed flow velocities and lower oxygen concentrations which are beyond the uniform flame border.

Also shown in Fig. 6 are the results of NCA experiments (Wang et al. 2016a; Zhu et al. 2016). A flammability map, including the uniform flame regime, flamelet regime and extinction regime is also presented. However, the extinction boundary and the uniform/flamelet boundary are all shifted to lower oxygen concentrations. Flame separation behavior occurs in lower oxygen concentration, leading to a narrow flamelet regime.

Flame Spread Rate

Flame spread rates are determined from the top view images for each test. The positions of flame and flamelet leading edges are tracked frame by frame. The time-history of the leading edge positions are fitted to a line with the least square technique. Then the slop of the fitted line is determined as flame spread rate. Measured flame spread rate as a function of gas flow velocity in microgravity, together with previously reported NCA forced convective data (Wang et al. 2016a; Zhu et al. 2016) are presented in Fig. 7. It is found that for both facilities, flame spread rate depends on the flow velocity and oxygen concentration with an increasing tendency. Although the data show a similar trend as the flow velocity increases, the spread rates in the NCA are several times higher than that in microgravity, especially at lower flow velocities. Considering the fact that the flame is sensitive to a small variation of oxygen supply at low flow velocities, one possible factor that could explain this distinction is the residual buoyant flows in the NCA, whose effect will be discussed in the next section.

Discussion

Flame and flamelet behaviors at low flow velocity are experimentally studied in two facilities. Good agreement is found between variation trend of flame and flamelet spread rate with flow velocity. A flammability map, constituted by three flame spread modes, is presented for both facilities. Results showed that significant information about flame spread over thermally thick solid fuels in low-velocity flows can be provided in the NCA. However, the residual buoyant flow in the NCA may be the main factor to cause the deviation of the flame spread rates in these two facilities. Olson et al. (2009) computed the characteristic flow velocity in the NCA using a heated wall section to simulate the flamelets. It was found that in a narrow channel with a height of 10 mm, the order of the magnitude of the buoyant velocity is about 1 cm/s, and when the inlet flow velocity is less than 5 cm/s, the buoyancy may play a significant role. Ren et al. (2011) performed a detailed numerical modeling of the flame spread over thermally-thin solid fuel in the NCA with a height of 10 mm. The buoyant flow velocity is estimated to about 5 cm/s. The slight buoyancy makes the NCA simulate flame spread in the low-velocity opposed flow in a qualitative manner with a probably reasonable result. However, the effect of buoyant flow on the flame spread is very complex, depending on both oxygen concentration and inlet flow velocity. In addition, in the horizontal narrow channel, the buoyant flows in the vertical direction, perpendicular to the direction of the forced flow. Therefore, the interaction of the buoyant flow and forced flow makes the flow in the channel complicated. This influence can be confirmed by the fact that the exact microgravity borders, as shown in Fig. 6, should shift right and upward relative to the NCA.

In order to better simulate flame spread in the NCA, the optimum gap height should be found to achieve the best compromise between heat loss and buoyancy suppression in the NCA. In order to assure a flame spreading in a channel, the channel height, L, should be higher than flame standoff distance, L_x. Otherwise, flame will extinguish. However, the gap height should be less than the total height, L_h , that is the sum of flame standoff distance and flame height. Higher gap height prevents the NCA from suppressing buoyancy. In the range of $L_x < L < L_h$, the heat loss to the boundaries should also be considered. Excessive heat loss to the boundaries will lead to large deviation especially in the low-velocity gas flow near the quenching limit.

Conclusions

Results of space-based microgravity experiments for flame spread over thermally-thick PMMA in varying low-velocity opposed-flows and ambient oxygen concentrations are reported. The experimental results are further compared with the counterparts in NCA tests conducted in normal gravity. Major conclusions are made as follows:

1. In a microgravity environment, uniform flame can sustain at high oxygen concentration, while at lower oxygen concentration and flow velocity only flamelets can survive. Both flame and flamelet have a steady spread rate. The spread rate increases with the increasing oxygen concentration and opposed flow velocity.
2. Flammability boundaries for thick PMMA are established using the microgravity data, which delineate uniform flame regime, flamelet regime and extinction regimes for thick PMMA fuels as a function of opposed flow velocity and oxygen concentration. The flammability area is extended to lower oxygen concentrations and lower opposed flow velocities by the flamelet.
3. Flame and flamelet behaviors in NCA qualitatively agree with that in microgravity. However, the flame spread rate and flammable range are overestimated in the NCA. The details of flamelet formation process are different. These findings enlighten us that more works should be done to improve the NCA performance in producing a microgravity flame spread environment for thick solid fuels.

Funding Information The work is funded by the National Natural Science Foundation of China, under grant No. U1738117, and the Strategic Pioneer Program on Space Science, Chinese Academy of Sciences, under grant No. XDA04020410.

References

Altenkirch, R.A., Tang, L., Sacksteder, K., Bhattacharjee, S., Delichatsios, M.A.: Inherently unsteady flame spread to extinction over thick fuels in microgravity. Proc. Combust. Inst. **27**, 2515–2524 (1998)

Fujita, O.: Solid combustion research in microgravity as a basis of fire safety in space. Proc. Combust. Inst. **35**, 2487–2502 (2015)

Hu, W.R., Zhao, J.F., Long, M., Zhang, X.W., Liu, Q.S., Hou, M.Y., Kang, Q., Wang, Y.R., Xu, S.H., Kong, W.J., Zhang, H., Wang, S.F., Sun, Y.Q., Hang, H.Y., Huang, Y.P., Cai, W.M., Zhao, Y., Dai, J.W., Zheng, H.Q., Duan, E.K., Wang, J.F.: Space program SJ-10 of microgravity research. Microgravity Sci. Technol. **26**, 159–169 (2014)

Ivanov, A.V., Balashov, Ye.V., Andreeva, T.V., Melikhov, A.S.: Experimental verification of material flammability in space. National Aeronautics and Space Administration NASA CR-1999-209405 (1999)

Matsuoka, T., Nakashima, K., Nakamura, Y., Noda, S.: Appearance of flamelets spreading over thermally thick fuel. Proc. Combust. Inst. **36**, 3019–3026 (2017)

Olson, S.L., Hegde, U., Bhattacharjee, S., Deering, J.L., Tang, L., Altenkirch, R.A.: Sounding rocket microgravity experiments elucidating diffusive and radiative transport effects on flame spread over thermally thick solids. Combust. Sci. Tech. **176**, 557–584 (2004)

Olson, S.L., Miller, F.J., Jahangirian, S., Wichman, I.S.: Flame spread over thin fuels in actual and simulated microgravity conditions. Combust. Flame **156**, 1214–1226 (2009)

Ren, T., Wang, S.F., Hu, J., Xiao, Y.: Study on flame spread over thermally thin fuels in narrow channel apparatus. J. Eng. Thermophys. **32**, 1617–1619 (2011). (in Chinese)

T'ien, J.S., Shih, H.Y., Jiang, C.B., Ross, H.D., Miller, F.J., Fernandez-Pello, A.C., Torero, J.L., Walther, D.: Mechanisms of flame spread and smolder wave propagation. In: Ross, H.D. (ed.) Microgravity Combustion: Fire in Free Fall. Academic Press, San Diego (2001)

Vietoris, T., Ellzey, J., Joulain, P., Mehta, S.N., Torero, J.L.: Laminar diffusion flame in microgravity: the minitexus 6 sounding rocket experiment. Proc. Combust. Inst. **28**, 2883–2889 (2000)

Wang, S.F., Zhu, F., Lu, Z.B.: Near-limit flame spread over thick solid fuels. J. Combust. Sci. Tech. **22**, 402–407 (2016a). (in Chinese)

Wang, S.F., Wang, S.D., Zhu, K.C., Xiao, Y., Lu, Z.B.: Near quenching limit instabilities of concurrent flame spread over thin solid fuel. Combust. Sci. Technol. **188**, 451–471 (2016b)

West, J., Tang, L., Altenkirch, R.A., Bhattacharjee, S., Sacksteder, K., Delichatsions, M.A.: Quiescent flame spread over thick fuels in microgravity. Proc. Combust. Inst. **26**, 1335–1343 (1996)

Zhang, X., Yu, Y.: Experimental studies on the three-dimensional effects of opposed-flow flame spread over thin solid materials. Combust. Flame **158**, 1193–1200 (2011)

Zhao, H.G., Qiu, J.W., Tang, B.C., Kang, Q., Hu, W.R.: The SJ-10 recoverable microgravity satellite of China. J. Space Explor. **4**(3), 101/1-9 (2016)

Zhu, F., Lu, Z.B., Wang, S.F.: Flame spread and extinction over a thick solid fuel in low-velocity opposed and concurrent flows. Microgravity Sci. Technol. **28**, 87–94 (2016)